

Quantum efficiency enhancement in film by making nanoparticles of polyfluorene

Ilkem Ozge Huyal, Tuncay Ozel, Donus Tuncel, and Hilmi Volkan Demir

Department of Physics, Department of Chemistry, Department of Electrical and Electronics Engineering, Nanotechnology Research Center, and Institute of Materials Science and Nanotechnology, Bilkent University, Bilkent, Ankara, Turkey 06800
volkan@bilkent.edu.tr and tuncel@fen.bilkent.edu.tr

Abstract: We report on conjugated polymer nanoparticles of polyfluorene that were formed to exhibit higher fluorescence quantum efficiency in film (68%) and reduce undesired emission peak wavelength shifts in film (by 20 nm), compared to the solid-state polymer thin film made directly out of the same polymer solution without forming nanoparticles. Using the facile reprecipitation method, solutions of poly[9,9-dihexyl-9H-fluorene] in THF were added at different volume ratios to obtain different size distributions of nanoparticle dispersions in water. This allowed us to control the size-dependent optical emission of our polyfluorene nanoparticles. Such organic nanoparticles hold great promise for use as efficient emitters in optoelectronic device applications.

©2008 Optical Society of America

OCIS codes: (250.0250) Optoelectronics; (250.3680) Light emitting polymers; (160.2540) Fluorescent and luminescent materials; (160.4890) Organic materials; (230.3670) Light-emitting diodes; Nanoparticles, size effect, fluorescence quantum efficiency.

References and Links

1. A. Charas, H. Alves, L. Alcacer, and J. Morgado, "Use of cross-linkable polyfluorene in the fabrication of multilayer polyfluorene-based light-emitting diodes with improved efficiency," *Appl. Phys. Lett.* **89**, 143519 (2006).
2. G. Heliotis, P. N. Stavrinou, D. C. C. Bradley, E. Gu, C. Griffin, C. W. Jeon, and M. D. Dawson, "Spectral conversion of InGaN ultraviolet microarray light-emitting diodes using fluorene-based red-, green-, blue-, and white-light-emitting polymer overlayer films," *Appl. Phys. Lett.* **87**, 103505 (2005).
3. H. V. Demir, S. Nizamoglu, T. Ozel, E. Mutlugun, I. O. Huyal, E. Sari, E. Holder, and N. Tian, "White light generation tuned by dual hybridization of nanocrystals and conjugated polymers," *New J. Phys.* **9**, 362 (2007).
4. A. Charas, J. Morgado, J. M. Martinho, A. Fedorov, L. Alcecer, and F. Cacialli, "Excitation energy transfer and spatial exciton confinement in polyfluorene blends for application in light-emitting diodes," *J. Mater. Chem.* **12**, 3523-3527 (2002).
5. I. O. Huyal, T. Ozel, U. Koldemir, S. Nizamoglu, D. Tuncel, and H. V. Demir, "White emitting polyfluorene functionalized with azide hybridized on near-UV light emitting diode for high color rendering index," *Opt. Express* **16**, 1115-1124 (2008).
6. I. O. Huyal, U. Koldemir, T. Ozel, H. V. Demir, and D. Tuncel, *J. Mater. Chem.* **18**, 3568 - 3574 (2008).
7. S. C. J. Meskers, J. Hübner, M. Oestreich, and H. Bassler, "Time-resolved fluorescence studies and Monte Carlo simulations of relaxation dynamics of photoexcitations in a polyfluorene film," *Chem. Phys. Lett.* **339**, 223-228 (2001).
8. A. Haugeneder, U. Lemmer, and U. Scherf, "Exciton dissociation dynamics in a conjugated polymer containing aggregate states," *Chem. Phys. Lett.* **351**, 354-358 (2002).
9. J. Gierschner, H.-J. Egelhaaf, D. Oelkrug, and K. Müllen, "Electronic deactivation and energy transfer in doped oligophenylenevinylene nanoparticles," *J. Fluorescence* **8**, 37-44 (1998).
10. I. B. Martini, A. D. Smith, and B. J. Schwartz, "Exciton-exciton annihilation and the production of interchain comparing the ultrafast stimulated species in conjugated polymer films: emission and photoluminescence dynamics of MEH-PPV," *Phys. Rev. B* **69**, 035204 (2004).
11. F. B. Dias, A. L. Macanita, J. S. de Melo, and H. D. Burrows, "Picosecond conformational relaxation of singlet excited polyfluorene in solution," *J. Chem. Phys.* **118**, 7119-7126 (2003).
12. T. Kietzke, D. Neher, K. Landfester, R. Montenegro, R. Güntner, and U. Scherf, "Novel approaches to polymer blends based on polymer nanoparticles," *Nature* **2**, 408-412 (2003).

13. N. Kurokawa, H. Yoshikawa, N. Hirota, K. Hyodo, and H. Masuhara, "Size-Dependent Spectroscopic Properties and Thermochromic Behavior in Poly(substituted thiophene) Nanoparticles," *ChemPhysChem* **5**, 1609-1615 (2004).
14. C. Syzmanski, C. Wu, J. Hooper, M. A. Salazar, A. Perdomo, A. Dukes, and J. McNeill, "Single Molecule Nanoparticles of the Conjugated Polymer MEH-PPV, Preparation and Characterization by Near-Field Scanning Optical Microscopy," *J. Phys. Chem B* **109**, 8543-8546 (2005).
15. F. Kong, Y. M. Sun, and R. K. Yuan, "Enhanced resonance energy transfer from PVK to MEH-PPV in nanoparticles," *Nanotechnol.* **18**, 265707 (2007).
16. F. Kong, X. L. Wu, G. S. Huang, R. K. Yuan, and P. K. Chu, "Tunable emission from composite polymer nanoparticles based on resonance energy transfer," *Thin Sol. Films* doi:10.1016/j.tsf.2007.12.055 (2008).
17. X. Wang, J. Zhuang, Q. Peng, and Y. Li, "A general strategy for nanocrystal synthesis," *Nature* **437**, 121-124 (2005).
18. F. Wang, M.-Y. Han, K. Y. Mya, Y. Wang, and Y.-H. Lai, "Aggregation-Driven Growth of Size-Tunable Organic Nanoparticles Using Electronically Altered Conjugated Polymers," *J. Am. Chem. Soc.* **127**, 10350-10355 (2005).
19. C. Wu, H. Peng, Y. Jiang, and J. McNeill, "Energy Transfer Mediated Fluorescence from Blended Conjugated Polymer Nanoparticles," *J. Phys. Chem B* **110**, 14148-14154 (2006).
20. H. Kasai, H. S. Nalwa, H. Oikawa, S. Okada, H. Matsuda, N. Minami, A. Kakuta, K. Ono, A. Mukoh, and H. Nakanishi, "A Novel Preparation Method of Organic Microcrystals," *Jpn. J. Appl. Phys.* **31**, L1132-L1134 (1992).
21. H. Kasai, H. Kamatani, S. Okada, H. Oikawa, H. Matsuda, and H. Nakanishi, "Size-Dependent Colors and Luminescences of Organic Microcrystals," *Jpn. J. Appl. Phys.* **35**, L221-L223 (1996).
22. C. Wu, C. Syzmanski, and J. McNeill, "Preparation and Encapsulation of Highly Fluorescent Conjugated Polymer Nanoparticles," *Langmuir* **22**, 2956-2960 (2006).

Fluorene-based polymers have been extensively investigated because of their superior optoelectronic properties to be utilized in various photonic device applications [1-6]. Of such π -conjugated systems, poly(9,9-dialkylfluorene)s are particularly attractive as blue emitters in organic light emitting diodes (OLEDs), thanks to their high quantum efficiency, ease of processability, and good thermal stability [2]. For use in such devices, it is necessary to deposit solutions of π -conjugated polymers onto solid substrates, typically by spin-coating, dip-coating, or drop-coating. This leads to electronic coupling of the polymer chains (interchain interaction), which is essential for charge carrier transport in the film state. Also, the presence of interchain coupled states induces an efficient energy transfer from higher energy intrachain singlet excitons to lower lying eigenstates that are delocalized over several polymer chains in intimate contact with each other (through dispersive relaxation processes). However, such aggregate-induced depopulation of the initially excited intrachain excitons also undesirably result in a significant red shift in the emission band, accompanied with a substantial reduction in the fluorescence quantum efficiency (Φ_{PL}) of typically more than 50% in the film state [7-11]. In this work, to address this problem, we propose and demonstrate the formation of organic nanoparticles (NPs) from π -conjugated polymers to exhibit higher fluorescence quantum efficiencies and reduced shifts in their emission bands in their NP films compared to their polymer thin films without forming NPs.

In the recent reports, various methods have been previously shown for the formation of organic NPs [12-21]. These include mini-emulsion process [12], hydrothermal synthesis [17], and reprecipitation [13,14,18-21]. Among them, especially attractive is the reprecipitation method because of its simplicity and versatility. This method involves the dissolution of a hydrophobic polymer in a good solvent and subsequent addition of the solution into a poor solvent to form folded polymer chains as nanoparticles. Previously, Masuhara et al. reported blue-shifting absorption and emission spectra as the diameters of P3DDUT (poly(3-[2-(N-dodecylcarbamoyloxy)ethyl]-thiophene-2,5-diyl) NPs were reduced from 420 nm to 40 nm [13]. This was attributed to polymer conformations, spatial arrangements, and lattice softening, which was also earlier proposed by Kasai et al. [13,21]. In another study on PFO (poly(9,9-dihexylfluorenyl-2,7-diyl), PFPV ({9,9-dioctyl-2,7-divinylene-fluorenylene}-alt-co-{2-methoxy-5-(2-ethylhexyloxy)-1,4-phenylene}), and MEH-PPV (poly[2-methoxy-5-(2-ethylhexyloxy)-1,4-phenylenevinylene]) NPs, McNeill et al. reported a blue shift in the absorption spectra but a red shift in the fluorescence spectra of their NP dispersions with

respect to their THF solutions, citing a quantum yield level of 10% for these NP dispersions [19,22].

In this paper, for the first time, we present highly efficient organic nanoparticles made of the polyfluorene derivative poly[9,9-dihexyl-9H-fluorene] (PF) ranging from 5 nm to 70 nm in diameter prepared by the reprecipitation method. We investigate the size-dependent optical behavior of these PF NPs at their different stages of processing, including their NP dispersions and their NP films, and comparing them against their original polymer stock solutions before NPs are formed and their polymer thin films made directly out of the same stock solutions without forming NPs. This provides a complete comparative study of modification to the optical emission properties including electronic transition wavelengths and fluorescence quantum efficiencies, during the entire processing of PF from stock solution synthesis to NP dispersion formation to NP film formation.

We use the synthetic pathway for poly[9,9-dihexyl-9H-fluorene] as described in our previous work [6]. Here in this work, first making NP dispersions and then their NP films, we discover that our nanoparticles with a relatively smaller size distribution (up to 30 nm in diameter) possess a high fluorescence quantum efficiency of $\Phi_{\text{PL}}=68\%$ in the film state, while relatively larger NPs (up to 70 nm in diameter) exhibit a comparatively lower fluorescence quantum efficiency of $\Phi_{\text{PL}}=43\%$, again in the film state. Particularly, the quantum efficiency of small NPs significantly surpass the efficiency observed for the solid state thin films of PF (without forming nanoparticles), which is typically in the range of 23-44% depending on the film thickness. This low quantum efficiency is closely related to the lower emission from the interchain aggregate species in the PF thin films.

As another interesting feature of PF NPs, we also observe that the spectral shifts in the emission peak wavelengths are greatly reduced for these nanoparticles when transformed from the dispersion to the film state. Though we observe an immense change in the fluorescence peak of the PF control group solution (emitting at 418 nm) when its solid film is formed (emitting at 450 nm), we do not observe such a significant change in the optical absorption spectrum. This confirms that the conformational changes within the polymer matrix do not affect the absorption properties to as great extent as the fluorescence properties. This indicates that, though material folding does not substantially affect the absorption, the fluorescence is diminished mainly due to increasing competitive non-radiative decay processes, arising from an increased number of polymer chains in close contact with each other. The optical emission properties of the polymer nanospheres are strongly dependent on their size, which we control by varying the injection volumes of the polymer solution relative to the volume of water. In this work, we use volume ratios of PF solution in THF to water to be 1/32 for small nanoparticles (SNP) and 1/4 for large nanoparticles (LNP) and prepare their solid state films by drop-casting. Figure 1 depicts the normalized absorption and photoluminescence (PL) spectra of PF stock solution and its thin film as the control group in (a), and those of the large and small PF nanoparticles in their NP dispersion and NP film states in (b) and (c), respectively.

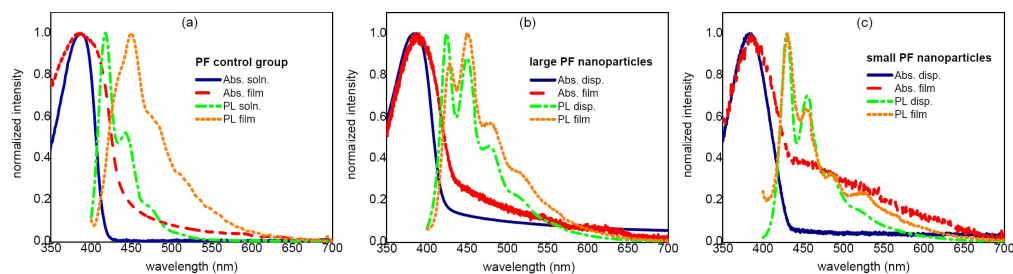


Fig. 1. Optical absorption and photoluminescence spectra of PF in different forms: (a) stock solution and polymer thin film as the control group, (b) large nanoparticle (LNP) dispersion and LNP film, and (c) small nanoparticle (SNP) dispersion and SNP film.

Small nanoparticles in dispersion have an absorption peak at 384 nm and emission peaks at 430 nm for the 0-0 electronic transition band, at 455 nm for the first vibronic side band (0-1 transition), and at 485 nm for the second vibronic side band (0-2 transition). On the other hand, large nanoparticles in dispersion have an absorption peak at 386 nm and emission peaks at 425 nm, 450 nm, and 477 nm for the 0-0, 0-1, and 0-2 electronic transitions, respectively. As far as the absorption spectra of PF control solution versus NP dispersions are concerned, we observe almost no change in the absorption peaks shown in Fig. 1, as also presented in their molar absorption coefficients in the onset of Fig. 2(a) to observe the effect of forming nanoparticle dispersions from the stock solution and in their film absorption coefficients in the inset of Fig. 2(a) to observe the effect of making solid state films. We observe scattering and reflection for the films of these nanoparticles and control group in the visible range, as presented in their transmittance spectra in Fig. 2(b). Here note that, in the atomic force microscopy (AFM) of these drop-coated solid state film samples in Fig. 2, NP film thicknesses are measured to be 35 nm for small nanoparticles and 83 nm for large nanoparticles, while the PF control film is 120 nm.

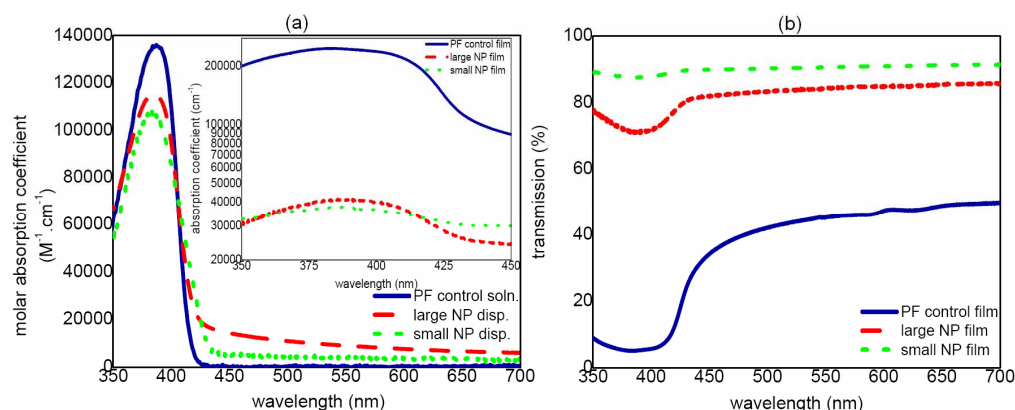


Fig. 2. Molar absorption coefficient of PF control solution and NP dispersions along with the absorption coefficient of PF control film and NP films in the inset (semi-logarithmic scale) and (b) transmittance spectra of PF control film and NP films.

The photoluminescence emission peaks, however, change significantly from 418 nm to 430 nm for SNPs and 425 nm for LNPs (Fig. 1) due to initial increase in the intramolecular interactions among polymer chains when NP dispersions are formed from the solution, while contrary to the transition from PF solution to its film, we do not expect any further red-shifting emission as films are formed from these NP dispersions. At shorter wavelengths (at higher photon energies), we notice a dominant contribution of the radiative decay from the intrachain excitons. But starting from around 525 nm, we observe broad emission, which is attributed to the radiative decay from excited interchain states populated within the initially excited high energy intrachain species. This observation is also verified by a close inspection of the full width at half maximum (FWHM) of emission bands in the PF solution, PF NP dispersion, PF thin film and PF NP film as listed in Table 1. The high intensity and sharpness of 0-0 transition both in the NP dispersion and in the NP film with the same FWHM of approximately 14 nm indicates that the radiative decay process takes place mainly through the excitation of high-lying intrachain states. This is further expected to induce at relatively low ratios the population of low-lying aggregate states constituting the outer structure of the nanoparticles at around 525 nm via energy transfer. This process shows itself with an increased FWHM wider than 70 nm around 525 nm.

Table 1. Peak emission wavelengths (λ) and full width at half maximum (FWHM) of the first (0-0), second (0-1), third (0-2), and fourth (0-3) emission bands of PF solution, PF thin film, PF large nanoparticle (LNP) dispersion, PF LNP film, PF small nanoparticle (SNP) dispersion, and PF SNP film.

(in nm)	λ_{0-0}	FWHM	λ_{0-1}	FWHM	λ_{0-2}	FWHM	λ_{0-3}	FWHM
PF solution	417.46	17.42	444.10	25.58	475.94	21.37		
PF thin film	446.01	42.09	482.68	35.28	520.57	65.41		
LNP dispersion	425.38	14.17	450.64	23.77	481.08	27.93	517.62	63.76
LNP film	428.69	14.12	450.57	25.58	481.70	31.97	520.89	70.76
SNP dispersion	429.16	14.55	455.13	20.67	484.84	31.84	524.53	63.14
SNP film	430.19	19.69	455.22	25.45	486.02	21.47	523.65	91.72

Similarly, the 0-0 transition in the PF solution is quite sharp with a FWHM of 17 nm and there is almost no emission beyond 500 nm. This gives countenance to the fact that initially in solution the emission takes place merely through the radiative process of non-aggregate species, thus yielding an almost ideal case with a very high fluorescence quantum efficiency of $\Phi_{PL}=83\%$. However, the thin film formation directly from this PF stock solution undesirably results in a drastic increase in the FWHM of the 0-0 transition to 42 nm, accompanied by a bathochromic shift of 33 nm and a reduced $\Phi_{PL}=23-44\%$ depending on the film thickness. Also, the emission spectrum of the polymer thin film turns out to be structureless compared to its solution spectrum. This strongly supports that, upon thin film formation, the emission process is dominated by migration of photo-excitations to non-radiative quenching centers and energetically lower-lying aggregate states.

SNPs exhibit an emission peak at 430 nm both in dispersion and in film, while LNPs shift their emission peak only by 3 nm from 425 nm to 428 nm, when transferred from the dispersion to the film state. These changes observed in the emission peak while transferring NPs from dispersion to film is quite insignificant compared to the changes observed going from stock solution to thin film. Correspondingly, the fluorescence quantum efficiency of SNPs and LNPs is not strongly reduced going from stock solution to their respective NP films, maintaining a high level of $\Phi_{PL}=68\%$ for SNPs and $\Phi_{PL}=43\%$ for LNPs in the film. There is, however, a red shift of approximately 8-13 nm observed in the NP dispersions compared to the original polymer stock solution. This shift is again insignificant compared to the shift of 33 nm observed going from the polymer solution to the polymer thin film. This red shift of the nanoparticles can be attributed to the initial collapse of hydrophobic polymer chains into compact nanostructures. For very dilute aqueous dispersions of the polymer nanoparticles, the interactions between different chains are minuscule, while interactions within the same chain at different segments increase. Thus, the non-radiative losses resulting from intrachain folding, which provides an alternative pathway for decay processes, are the main reason for the reduced quantum efficiency with respect to the solution state.

We discussed that once folding of polymer chains into nanoparticles takes place, their emission spectra are red-shifted by 8-13 nm depending on the particle size with respect to PF in THF. Here a difference of 5 nm in emission peak wavelengths of SNPs versus LNPs arises from the stronger contribution of red-shifted intramolecular forces acting in SNPs yielding a larger red-shift. On the other hand, in LNPs we obtain a less compact structure so that the emission of high-lying intrachain species is not red-shifted to an equally large extent. Thus, the more blue-shifted emission appears at 425 nm.

The nanoparticle formation thus provides a convenient pathway for the elimination of interchain effects. As a result, the observed optical properties can be directly associated with the intrachain interactions in the small-sized nanoparticles, which implies almost identical optical behavior of collapsed nanoparticles in the dispersion and film states as is verified from the emission spectra in Fig. 1. Since there are no additional non-radiative mechanisms, PF nanoparticle films in turn lead to much higher Φ_{PL} than PF thin films. A schematic

comparative representation of PL shifts going from PF solution to PF thin film and from the same PF solution to PF NP dispersion to PF NP film is given in Fig. 3, where red and blue arrows indicate red- and blue-shifts with respect to their previous states, respectively. As clearly observed in Fig. 3, from optical perspective, as opposed to making thin polymer films directly out of the stock solution, it seems to be a better route to get at the final film state via nanoparticle formation to reduce the PL shifts with respect to the starting stock solution and maintain high fluorescence quantum efficiency.

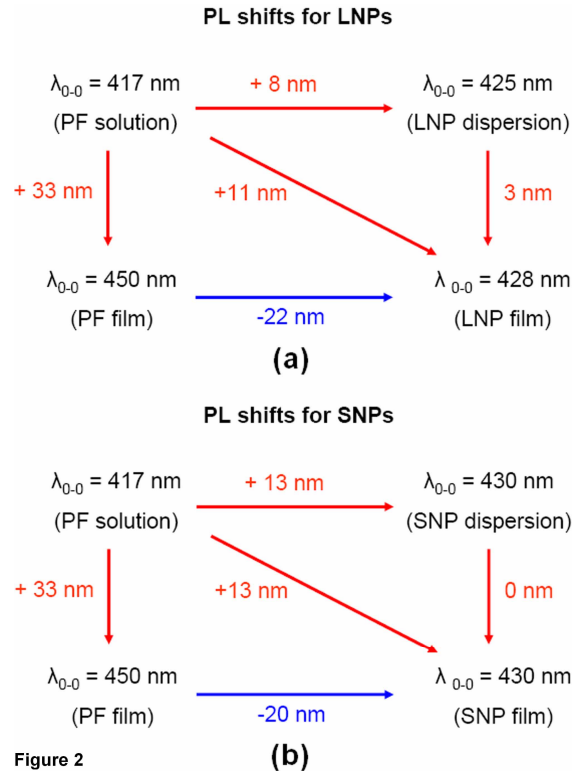


Figure 2

Fig. 3. Spectral PL shifts for 0-0 electronic transition of PF LNPs (large nanoparticles) and SNPs (small nanoparticles) in their dispersion and film states relative to their stock solution and polymer thin films.

Collapse of polymer chains into nanoscale spherical particles results in a reduction of the conjugation length by bending or kinking of the polymer backbone. Thus, we expect slightly blue-shifted absorption spectra especially in the small nanoparticles. Competitively, morphological changes such as increased chain-chain packing lead to red-shifting absorption spectra, which becomes especially a prominent effect for larger nanoparticles. Also the molar absorption coefficients decrease for smaller nanoparticles, which is an effect related to the morphological changes and the resulting scattering. Though scattering is a minor issue in dispersions of NPs, we observe a noteworthy increase of scattering in NP films compared to their dispersion. Although the observed decrease in the absorption coefficient with smaller nanoparticles decreases the absorption of incident light, the overall high quantum efficiency shows that well-isolated small nanoparticle formation is a competent method to overcome this deficiency and achieve highly increased photon conversion. To show the difference in the lateral size distribution of such smaller and larger nanoparticles, Fig. 4 presents the AFM topography of some exemplary SNP and LNP films, indicating a lateral diameter range of 5-30 nm for SNPs and 5-70 nm for LNPs. Here Fig. 4(a) also shows that monodispersity cannot be achieved at higher concentrations.

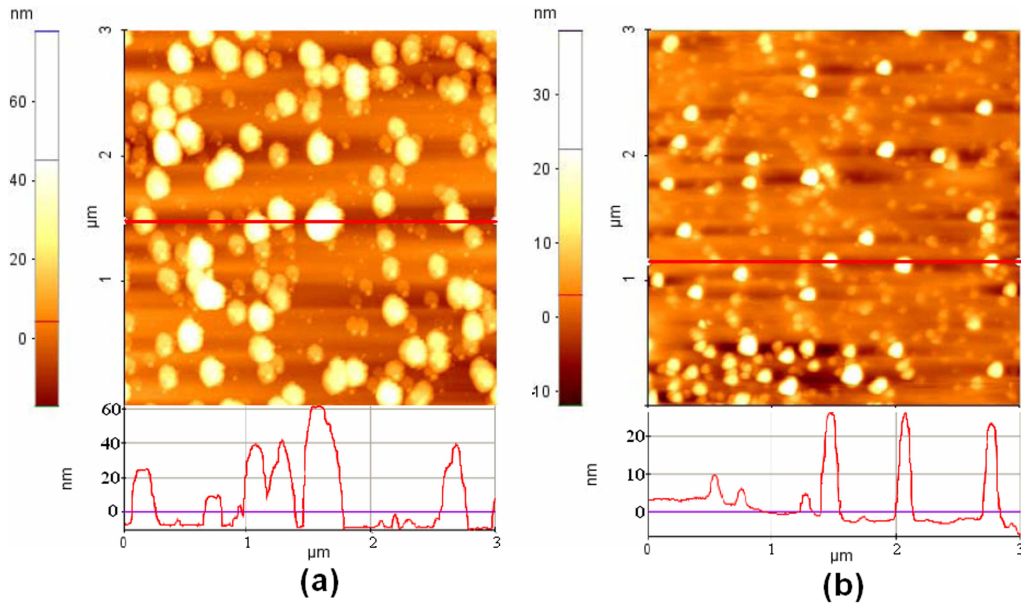


Fig. 4. AFM images and line profiles for PF LNPs and SNPs with size distributions ranging from 5-70 nm and 5-30 nm, respectively.

In conclusion, we presented highly efficient nanoparticles of polyfluorene with a relatively small size distribution of 5-30 nm and a relatively large distribution of 5-70 nm in diameter. We observed high fluorescence quantum efficiencies for the NP films at 68% for SNP and 43% for LNPs, unlike the bulk thin film of PF, which can be as low as 23% depending on the film thickness. Furthermore, we reported a significant reduction in PL peak emission shift of about 20 nm in the NP films compared to the polymer thin film. Nanoparticle formation reduces the PL shifts with respect to the starting stock solution, while maintaining high fluorescence quantum efficiency in the film. From optical point of view, nanoparticle formation offers an alternative route to make efficient films as opposed to the conventional approach of using the stock solution directly to make thin films. For the electronic perspective, the investigation of carrier injection into these nanoparticles is currently in progress. From optical perspective, our initial experiments indicate that such organic nanoparticles hold great promise for use as efficient emitters in future OLEDs.

Acknowledgment

This work is supported by EU-PHOREMOST NoE 511616 and EU Marie Curie IRG MOON 021391, and TUBITAK 106E020, 105M027, 104E114, 107E088, 107E297, 105E065, and 105E066. Also, HVD acknowledges additional support from European Science Foundation (ESF) European Young Investigator Award (EURYI) and Turkish Academy of Sciences (TUBA) Distinguished Young Scientist Award (GEBIP) Programs.